Chemical Engineering Journal 160 (2010) 340–350

Contents lists available at ScienceDirect

Chemical Engineering Journal

journal homepage: www.elsevier.com/locate/cej

Chemical modification of P84 polyimide as anion-exchange membranes in a free-flow isoelectric focusing system for protein separation

Jiu-Hua Cheng, You-Chang Xiao, Cuiming Wu, Tai-Shung Chung*

Department of Chemical and Biomolecular Engineering, National University of Singapore, 10 Kent Ridge Crescent, Singapore 119260, Singapore

ARTICLE INFO

Article history:
Received 23 September 2009
Received in revised form 9 February 2010
Accepted 25 February 2010

Keywords:
Protein separation
Ion exchange membrane partitioned
free-flow isoelectric focusing (IEM-FFIEF)
pH gradient
Electrophoresis
Ion exchange membrane

ABSTRACT

By means of amination with diamine and methylation with methyl iodide, we have modified P84 microporous polyimide membranes with characteristics of highly charged anion-exchange membranes. FTIR (Fourier transform infrared-attenuated total reflection) and XPS (X-ray photoelectron spectroscopy) confirm the amination and methylation reactions on membrane surfaces. The intrinsic properties of the newly developed anion-exchange membranes have been fully characterized in terms of ζ-potentials, electrical resistances, PWPs (pure water permeation) and pore size distributions. By using the newly developed membranes, a free-flow isoelectric focusing (IEM-FFIEF) has been set up for the separation of myoglobin (Mb) and lysozyme (Lys) mixtures. Experimental data show that (1) the Mb flux via the highly charged P84 anion-exchange membrane can be 10 times higher than that of the original P84 membrane and (2) the high surface charge is the predominant factor for the enhanced Mb flux. HPLC (high performance liquid chromatography) results show that not only the Mb flux was high, but also its purity in the permeate side is extremely high. It is therefore concluded that the diamine and methyl iodide modifications can effectively modulate P84 nano-porous membranes with anion-exchange characteristics, which is suitable for the IEM-FFIEF application.

1. Introduction

The demand of pure protein products has been increasing rapidly which triggers the research of more efficient technologies for protein separation. Many technologies for protein separation have been developed such as chromatography, crystallization, moving bed column, electrodialysis, electrophoresis, membrane ultrafiltration and membrane chromatography, etc. Among them, membrane based protein separation is believed possible to meet the industrial demands on high throughput and high selectivity [1]. However, the surface charge characteristics of proteins make protein separation through a membrane complicated, because of the electrostatic interactions between solute molecules and membrane pore surfaces.

The basic theory of long-range colloidal interactions (electrostatic effect) between a protein solute and membrane pores has been developed by Smith and Deen [2,3]. Taking the advantage of electrostatic interaction, Zydney and co-workers have developed pioneering technologies for membrane based protein separation [4,5]. Meanwhile, other scientists also reported enhanced protein separation with the aid of electric driving force applied across the membrane [6–9], e.g. the membrane based electrodialysis systems and the electrophoretic membrane contactors. Of all known electrophoretic methods, the isoelectric focusing (IEF) gains the highest resolution [10]. Recycling isoelectric focusing (RIEF) was therefore developed to concentrate charged macro-molecules at specific locations with pH equals to their pI values [10,11]. The RIEF can be designed with or without porous screens as partition media between chambers. Bier and co-workers were the pioneers innovated the screened RIEF, e.g. Rotofor, which has been commercialized by Bio-Rad Laboratories, for lab-scale protein fractionation. However, the screens used in their design have big pores that can only reduce the convective flow between chambers but not confine specific protein molecules in a narrow range, for example in one chamber. Thus in the Rotofor device, separated proteins are distributed in a range of neighborhood chambers. On the other hand, since the turbulent flow is inevitable in a big scale process, the non-specific distribution of protein products is an issue and will increase production cost for further purification. Therefore, we propose using ion-exchange membranes with tailored pore sizes for FFIEF, because the permselectivity possessed by the membrane surface can simultaneously prevent the convective mixing and confine the separated protein in a specific chamber.

To obtain a high flux from FFIEF protein separation, the molecular design of ion exchange membranes with a suitable ion exchange capacity (IEC) and pore properties is essential [12,13].

* Corresponding author. Fax: +65 6779 1936.
E-mail address: chencts@nus.edu.sg (T.-S. Chung).

1385-8947/$ – see front matter © 2010 Elsevier B.V. All rights reserved.
doi:10.1016/j.cej.2010.02.058

Nomenclature

a	the particle radius
b	the pore radius
r	the size of molecules used in real solute rejection test
A	the cross-section area of the streaming channel of Anton Paar streaming potential analyzer
C_p	the concentration of permeat solution in real solute rejection test
C_f	the concentration of the feed solution in real solute rejection test
F_p	the percentage of pores above the effective pore size
L	the length of streaming channel of Anton Paar streaming potential analyzer
R	the electric resistance
R_T	the real solute rejection rate in real solute rejection test
T_g	the glass transmission temperature
U	the translation velocity of electrophoresis
dU/dP	the slope of streaming potential versus pressure
μ	the mobility
ε	the dielectric constant of buffer
ε_r	the relative dielectric constant
ε_0	the vacuum permittivity
η	the viscosity of buffer
λ	the ratio of particle radius a and pore radius b, $\lambda = a/b \ll 1$
ζ_s	the surface ζ-potential of solute
ζ_w	the surface ζ-potential of pore wall

To design a positively charged polymer, various chemical modifications have been published. They are (1) chloromethylation through chloromethylmethyl ether (CME) or bis-chloromethyl ether (BCME), followed by amination [14,15]; (2) bromination of benzyl group followed by amination [16,17]; (3) acetylation followed by amination [18–19]; (4) surface amination by ammonia plasma treatment [20]. However, the wet processes like the first three methods normally involve very toxic and carcinogenic reagents [21]. Bromination of PPO (poly(2,6-dimethyl-1,4-phenylene oxide)) needs boiling the bromine in a chlorobenzene solution at 131 °C, and both bromine and chlorobenzene are in the forbidden list of disposal in some countries [22]. For the fourth method, the high cost plasma-generator limits its extensive application.

An anion-exchange membrane has been developed in this work under milder operation conditions using a commercially available co-polymer P84 polyimide. P84 is a high temperature polyimide (glass transmission temperature T_g 315 °C, density 1.31 g/cm^3) with superior thermal and membrane structural properties [23–28]. As a member of polyimide family, it can react with amine for further modifications [27,28]. The modified membranes were then characterized by a series of analytic equipments and tested in the IEM-FFIEF system using a kinetic UV–vis spectrometer as an on-line process monitor. The purity of permeate products were measured by high performance liquid chromatography (HPLC).

2. Experimental

2.1. Experimental set-up

Combining the electrostatic effects between protein molecules and membrane pores, and the isoelectric focusing technology, we have designed an IEM-FFIEF (ion-exchange membrane partitioned

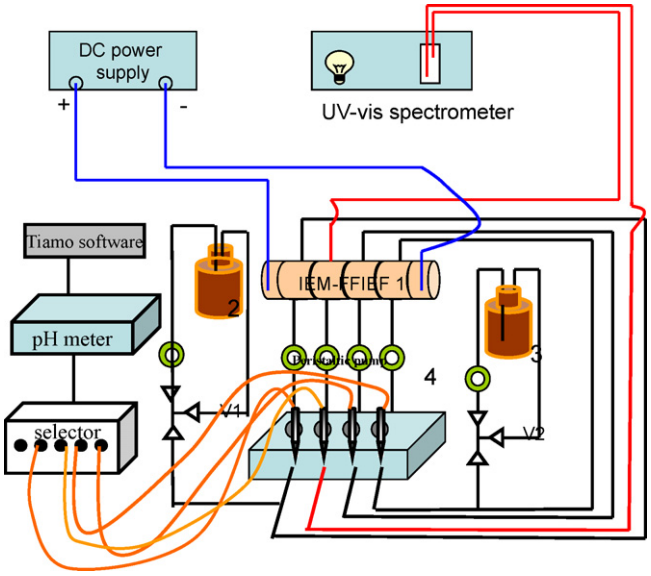

Fig. 1. Experimental set-up of the IEM-FFIEF system.

isoelectric focusing) system for bovine serum albumin (BSA) and hemoglobin (Hb) separation [12] as shown in Fig. 1. It consists of a FFIEF cell, power supply, circulation pumps, pH automation system and UV–vis spectrometer. Fig. 2 shows the details of the IEM-FFIEF cell. The electrode chambers were set at two ends and buffer chambers were inserted in between two electrode chambers. All of chambers were partitioned by the newly developed ion-exchange membranes to prevent the convective flow between chambers and to confine the separated proteins in specific chambers. Chambers 1, 2, 3 and 4 were fed in buffers with different pH values in a designed sequence as shown in Fig. 2. A quasi-stable pH gradient in a protein separation membrane (between chambers 2 and 3) was realized by adjusting pH values in chambers 1 and 4 at a stable level.

It has been well known that most proteins can be ionized under various pH as shown in Eqs. (1) and (2):

$$\text{For pH} < \text{pI} \quad \begin{matrix} \text{R–NH}_2 + \text{H}^+ \rightarrow \text{R–NH}_3^+ \\ \text{R–COO}^- + \text{H}^+ \rightarrow \text{R–COOH} \end{matrix} \tag{1}$$

$$\text{For pH} > \text{pI} \quad \begin{matrix} \text{R–NH}_3^+ + \text{OH}^- \rightarrow \text{R–NH}_2 + \text{H}_2\text{O} \\ \text{R–COOH} + \text{OH}^- \rightarrow \text{R–COO}^- + \text{H}_2\text{O} \end{matrix} \tag{2}$$

Therefore, the charged proteins show ionic characteristics under a wide range of pH. A protein can spontaneously move toward the location where the medium pH equals to its pI (isoelectric point) value and be stationary at that location. Thus the protein molecules can migrate across membranes and be relocated into different chambers according to their pI values. When a charged membrane is used, proteins would be rejected if the membrane surface has the same charge, while be adsorbed and/or migrate across the membrane under an electric field if the membrane surface has an opposite charge. It has been known that the interaction between protein molecules and membrane pore surface in electrophoresis is different from the phenomenon of electrostatic effects. In electrophoretic scope this interaction was called boundary effects which induced electrophoretic mobility, Poiseuille flow, electroosmotic flow, viscous retardation and the distorted electrostatic interaction between charged particles and pore surfaces arisen by applied electric fields [13].

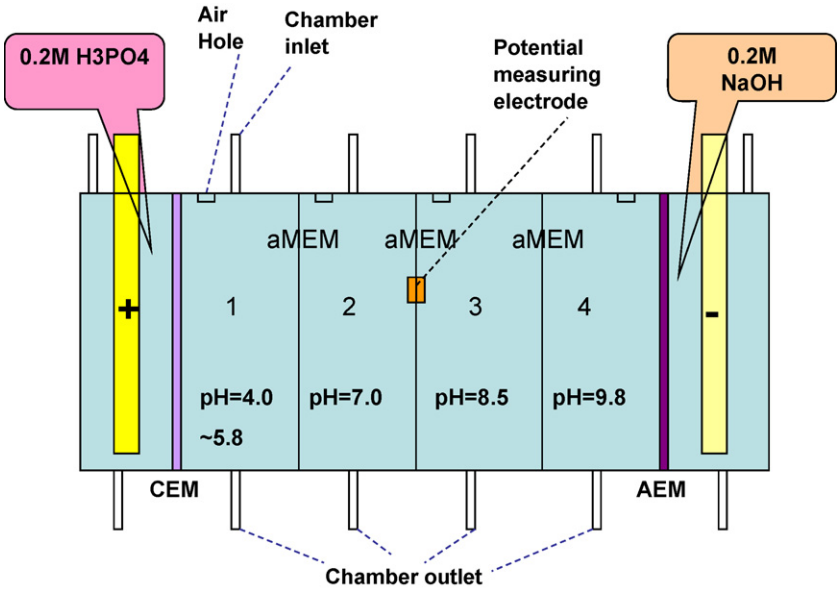

Fig. 2. Close up of the membrane partitioned isoelectric focusing cell.

2.2. Materials

The P84 co-polyimide as shown in Fig. 3 with a molecular weight (M_w) of 153 kDa [29] was obtained from HP polymer GmbH, Austria. myoglobin (Mb), lysozyme (Lys), ethylene diamine, diamine butane and polyethylene oxide (PEO), polyvinylpyrrolidone (PVP) were obtained from Sigma–Aldrich. The M_w and pI values of Mb are 17 kDa and 6.8, respectively; the M_w and pI values of Lysozyme are 14.4 kDa and 11.0, respectively. N-methyl-2-pyrrolidone (NMP), phosphoric acid (H_3PO_4), phenolphthalein, trifluoroacetic acid, acetic acid, methyl iodide (CH_3I), sodium hydroxide (NaOH), methanol and acetonitrile (ACN) were all provided by Merck. Tris was from Bio-Rad, and isopropanol (IPA) was from TEDIA Inc. Hydrochloric acid was purchased from Fisher Scientific. All of reagents except ACN were of AR (analytical reagent) grade. For HPLC, GR (guaranteed reagent) grade water from Merck was used, while for other occasions, deionized water (DI water, electrical resistance $R < 18.2\,M\Omega$) was used. The dense cation-exchange membrane and anion-exchange membrane (commercial name CEM, AHA) were purchased from Astom Corporation, Japan.

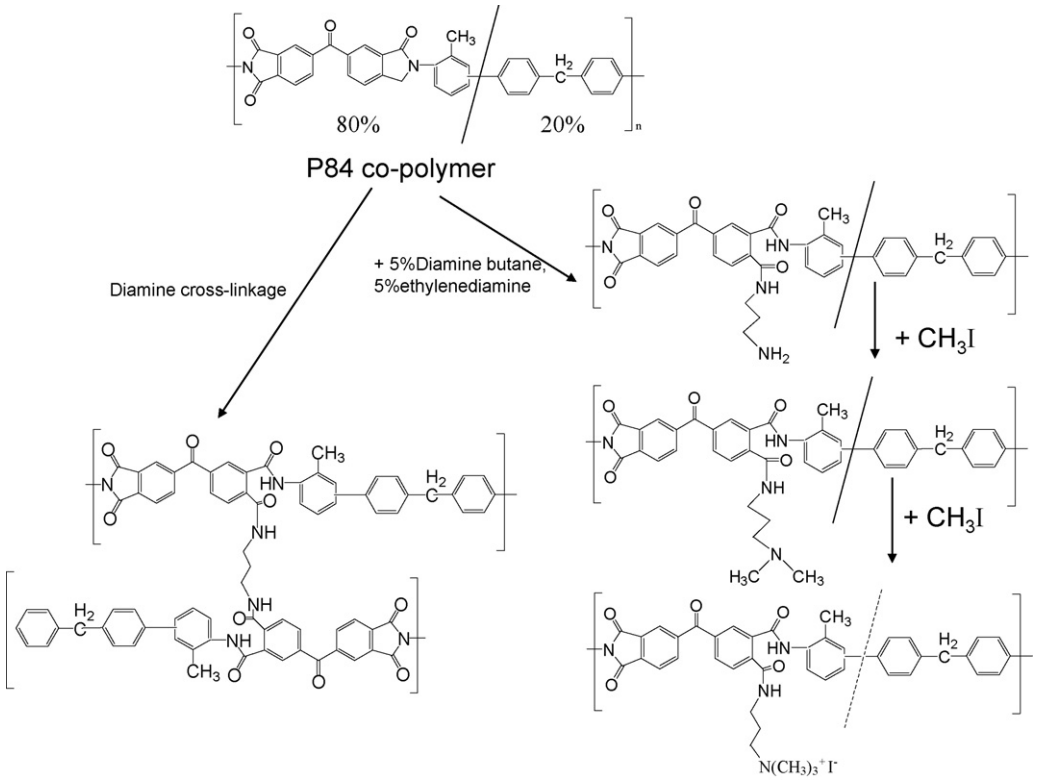

Fig. 3. Chemical structure and reactions of P84.

2.3. Preparation of P84 anion-exchange flat membranes

The P84 polymer was used to prepare anion-exchange membranes with the following procedures: (1) phase inversion: P84 powder was dissolved in NMP with a concentration of 23% (w/w). Then the solution was cast onto a piece of non-woven cloth by a casting blade with a gap thickness of 150 μm. The non-woven cloth was immediately immersed in IPA. After 20 min, it was taken out and immersed in methanol for 2 h. The P84 porous membrane as obtained was named M-0. (2) Amination with diamine: the M-0 membrane was directly soaked in a 5/5/90 (in V/V) ethylene diamine/diamine butane/methanol solution for 30 min. Capitalizing the porous nature of the membrane surface and the short length of the diamine molecules, some diamine will react for the cross-linkage [30], while some free-NH_2 groups will be remained which can be utilized for further methylation to form quaternary amine. Then the un-reacted diamine was removed by washing with methanol and the modified membrane was named M-1. (3) Methylation with methyl iodide: the M-1 membrane was subsequently dipped in a 20 wt% methyl iodide–methanol solution for 12 h. Methyl iodide is chosen for the preparation of quaternary amine salt because of its high reactivity for nucleophilic substitution [30]. Two different reaction temperatures, 42 °C or 48 °C, were applied and the obtained membranes were named M-2 and M-3 individually. The above amination and methylation processes are schemed in Fig. 3. (4) All of the membranes M-0, M-1, M-2 and M-3 were post-treated as per routine: soaking in 0.5 M HCl for 12 h followed by fully washing with DI water; soaking in 1 M NaCl solutions for 12 h followed by fully washing with DI water. As shown later, the membrane charging property increases with an increase in the degree of modification.

2.4. Membrane characterization

Fourier transform infrared-attenuated total reflection (FTIR-ATR) measurements were carried out using a Bio-Rad FTS 135 FTIR spectrometer to identify the changes of chemical structure of membrane surface in a wave-number range from 700 to 3000 cm^{-1}. XPS (X-ray photoelectron spectroscopy) measurements were applied to analyze the membrane surface modification through AXIS HSi spectrometer (Kratos Analytical Ltd. England). All core-level spectra were collected under 1486.6 eV photons and a photon electron takeoff angle of 90°. The morphologies of membranes were observed through a JSM-6700F FESEM (field emission scanning electron microscopy). Membrane samples were fractured in liquid nitrogen, dried under vacuum at room temperature and then coated with platinum before FESEM observation.

A streaming potential analyzer (Anton Paar GmbH) was used for surface charge characterization. As given by Helmholtz–Smoluchowsky method, the apparent ζ-potential can be measured through:

$$\zeta_{\text{apparent}} = \frac{dU}{dP} \times \frac{\eta}{\varepsilon_r \times \varepsilon_0} \times \frac{L}{A \times R} \quad (3)$$

where dU/dP is the slope of streaming potential versus pressure; η is the electrolyte viscosity; ε_r is the relative dielectric constant of electrolyte; ε_0 is the vacuum permittivity; L is the length of streaming channel; A is the cross-section area of the streaming channel; R is the resistance inside the measuring cell. The sample for streaming potential measurements was titrated from pH 10 to pH 4.5 in a HCl–tris buffer. This pH range covered all related pH values in the IEM-FFIEF separation process. A series of ζ-potential data were obtained as a function of pH. It must be noticed that in order to mimic the real situations on membrane surface during the protein separation process, the buffer solution in a streaming potential analysis was 20 mM HCl–tris solution, which led to much higher ζ-potential readings compared to the literature reports. The high apparent ζ-potential was due to the fact that in dilute solutions, such as 1 mM KCl or 20 mM HCl–tris buffers, the conductivity of charged surface was not negligible, thus the ζ-potential results needed to be corrected by 0.1 M KCl through Eq. (4) [31]:

$$\zeta_{\text{corrected}} = \frac{dU}{dP} \times \frac{\eta}{\varepsilon_r \times \varepsilon_0} \times \frac{\kappa_{0.1\text{ M KCl}} \times R_{0.1\text{ M KCl}}}{R} \quad (4)$$

where $\kappa_{0.1\text{ M KCl}}$ is the conductivity of 0.1 M KCl; $R_{0.1\text{ M KCl}}$ is the cell resistance when running 0.1 M KCl.

The ion-exchange capacities (IEC) were determined by the Mohr method [17,18]. A given area of the membrane was soaked in a 100 ml 0.1 M Na_2SO_4 solution for 24 h and the Cl^- concentration as released was tested by a Cl^- ion selective electrode. The IEC value was expressed as meq/m^2. The pure water permeation (PWP) test was performed under 5 bar. The electric resistance (R) was measured in a special measuring cell as follows. Membranes M-0, M-1, M-2 and M-3 were immersed in 0.1 M KCl for 24 h, followed by placing each one of them in an electrical testing cell in which the membrane was mechanically sandwiched and tightened. Then electric resistance was individually measured at 25 °C through a multi-meter.

The pore size distribution was measured by a real rejection method using a series of neutral molecules (PEG: 2 kDa; PVP: 10 k, 55 k, 360 k, 1300 kDa) with the aid of the following relationship between molecular weight and Stoke radius [32]:

$$\begin{aligned} &\text{For PEG,} \quad r = 16.73 \times 10^{-3} \times M_w{}^{0.557} \text{ nm} \\ &\text{For PVP,} \quad r = 8.40 \times 10^{-3} \times M_w{}^{0.593} \text{ nm} \end{aligned} \quad (5)$$

The given standard neutral molecules were prepared into 100 ppm mixtures and filtered through the membrane which was mounted in a permeation cell under a 5 bar pressure. Then the permeate and feed compositions were analyzed with the aid of GPC (Gel Permeate Chromatography) using a 25 cm PL-aquagel-OH mixed 8 μm column (Agilent). The real rejection rate is obtained from the integration area of individual peaks as follows:

$$R_T = \left(1 - \frac{C_p}{C_f}\right) \times 100\% \quad (6)$$

The real rejection rate as a function of molecular radius was further used to estimate the MWCO (molecular weight cut-off), mean pore size and pore size distribution according to the methods described elsewhere [32,33]. An Agilent technologies 1200 series high performance liquid chromatography (HPLC) instrument equipped with both a VWD and a RID detector was applied for PEG and PVP concentration tests through a GPC. The GPC was operated at the following conditions: pure water as solvent, 60 min running time, 0.5 ml/min flow-rate, and constant temperature at 30 °C.

In order to investigate the mechanical strength and stability of the modified membranes, a tensile testing machine INSTRON 5542 was used to measure the tensile strength and Young's modulus. The mechanical strength and stability of one set of the M-3 samples were tested after one week of operation without protein feed under the conditions listed in Fig. 2; while the other sets of M-3 samples were tested after immersing in 0.1 M HCl and water for two weeks, individually. All samples were cut into 5 mm widths, and the measuring lengths were all in 25 mm.

2.5. HPLC analyses of protein solution

High performance liquid chromatography (HPLC) was applied for the analysis of the concentration of individual protein. An Agilent technology 1200 HPLC with a VWD detector was used to determine the protein purity in the respective chambers. The C18 mass SPEC column was purchased from Grace Vydac Inc. The gradient elution was comprised by two mobile phases contained A: 100%

Table 1
Running conditions of HPLC.

HPLC Parameters	Controlled values
VWD wavelength	214 nm
Temperature	30 °C
Flow speed	1.0 ml/min
Running time	30 min
Post-time	5 min
Injection	100 μl

acetonitrile with 0.1% trifluoroacetic acid; B: 100% water with 0.1% trifluoroacetic acid. The protein sample analyses were conducted with the parameters as showing in Table 1.

2.6. Protein separation by anion-exchange membrane partitioned free-flow isoelectric focusing (IEM-FFIEF)

Figs. 1 and 2 show the experimental set-up for the IEM-FFIEF cell which includes two electrode chambers and four buffer chambers of different pHs: 4.0–5.8, 7.0, 8.5 and 9.8 individually. The effective separation areas for all ion exchange membranes were of 42.9 cm^2 and the chamber thicknesses were of 4.8 cm. The separation was running under a constant current of 100 mA. As shown in Fig. 2, dense cationic and anionic membranes were used between an electrode chamber and chamber 1 or 4 to avoid the protein molecules from attaching to the electrodes. A 200 ml protein mixture made of 500 ppm Mb and 500 ppm Lys was fed into chamber 3. Since chamber 3 had a pH value of 8.5 that was bigger than Mb's pI but smaller than Lys's pI, Lys molecules would carry positively charges and Mb molecules would carry negatively charges. Therefore, under an electric driving force, the negatively charged Mb would migrate through the positively charged anion-exchange membrane and go into chamber 2 (pH 7.0) and be stationary in chamber 2, this is because the surface charge of protein would reduce to zero when pH = pI. The concentration of chamber 2 would increase and the increment can be on-line monitored by a UV–visible spectrometer at the wavelength of 408 nm [34]. The protein concentrations of all chambers were then measured by a HPLC to verify the separation performance.

3. Results and discussion

3.1. Confirmation of the modification

After amination with diamine and methylation with methyl iodide as shown in Fig. 3, the as-cast P84 membranes were expected to exhibit characteristics of anion-exchange membranes. The FTIR-ATR spectra shown in Fig. 4 confirm the above reactions [35]. The strong and broad bands of imide groups of P84 at 1363, 1732 and 1781 cm^{-1} become significantly weakened after the diamine treatment, while a very weak new peak appears at 1650 cm^{-1}, which is due to the formation of –CO–NH– group [24–26,36]. Similarly after methylation reaction, amine salt forms and new peaks in the range of 1500–1550 cm^{-1} appear [36]. Moreover, $-CH_3$ groups absorption in the range of 2850–2921 cm^{-1} appear, which is associated with characteristics of $-CH_3$ groups in $-N(CH_3)_3^+ I^-$ [28,36], thus confirming the methylation and quaternary amination on P84 membranes.

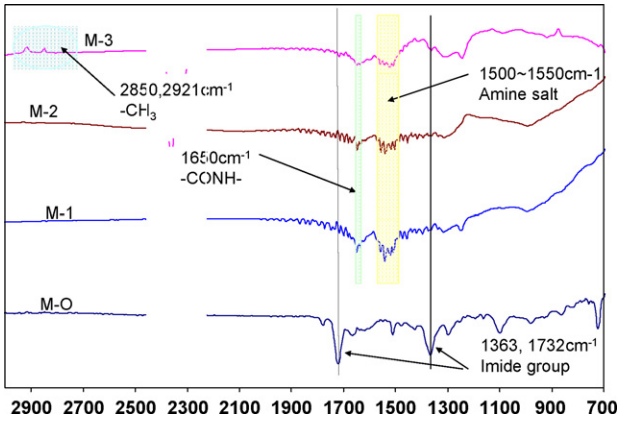

Fig. 4. FTIR-ATR spectra of the original P84 membrane M-0, diamine modified membrane M-1, methylated amine membrane M-2 and M-3.

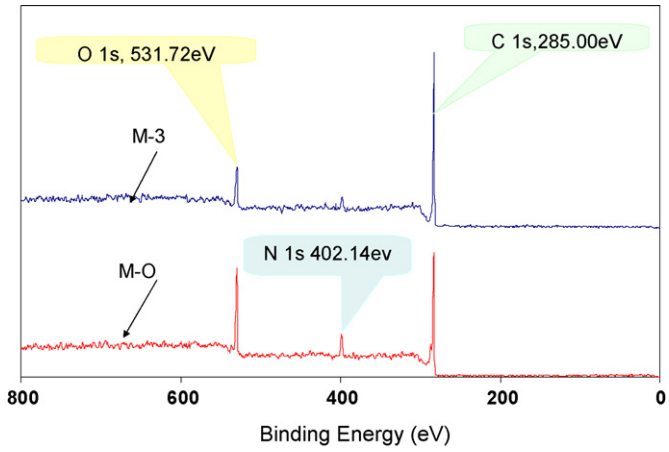

Fig. 5. Comparison of element ratio from wide scans of the original P84 membrane (M-0) and quaternary amine membrane (M-3).

Fig. 5 exhibits the element ratio of membranes M-0 and M-3 calculated from XPS spectra. Since the oxygen element remains the same chemical state and its amount is constant, while N and C elements change during the whole modification process, the changes in O:N:C ratio as shown in Fig. 5 and Table 2 confirm the modification reactions. The increased content of carbon element in M-3 indicates the quaternary amination occurring on the P84 membrane surface.

Fig. 6 shows the quantity and chemical states of C 1s core-level of different membrane surfaces. As pointed by Qiao and Chung [25], for the original P84 membrane, the bond at 284.6 eV is for C–H, at 285.8 eV is for C–N, at 288.4 is for $N(C{=}O)_2$ and at 291.1 eV is for aromatic ring. After modifications, compared with the original P84 membrane, the intensity of imide group, $N(C{=}O)_2$, of M-1 and M-3 has a visible decrease. Clearly, the imide groups have been partially reacted, whereas a new peak appears at 287.9 eV which is attributed to –CO–NH– groups as a reaction product between primary amine and imide groups [36]. When the M-3 is compared with the M-1, the ratio of the C–H peak to the $N(C{=}O)_2$ peak increases due to the methylation of free amino ends. Fig. 7 illustrates the quantity and chemical states of N 1s core-level of different membrane surfaces. The peak at 399.81 eV is due to –CO–NH–, whereas the peak at 402.14 eV is due to amine salts [36]. However, Fig. 7 seems to provide no help on distinguishing secondary, tertiary and quaternary amine salts, thus further characterization by streaming potential is needed to confirm the quaternary aminated surface.

Table 2
The XPS element analyses of the original P84 membrane and methylated amine membranes.

Element	Binding energy (eV)	M-0	M-2	M-3
O 1s	531.72	729	234	415.4
N 1s	402.14	294	117	213
C 1s	285.0	828	314	1172
O:N:C	–	1:0.4:1.14	1:0.5:1.34	1:0.5:2.82

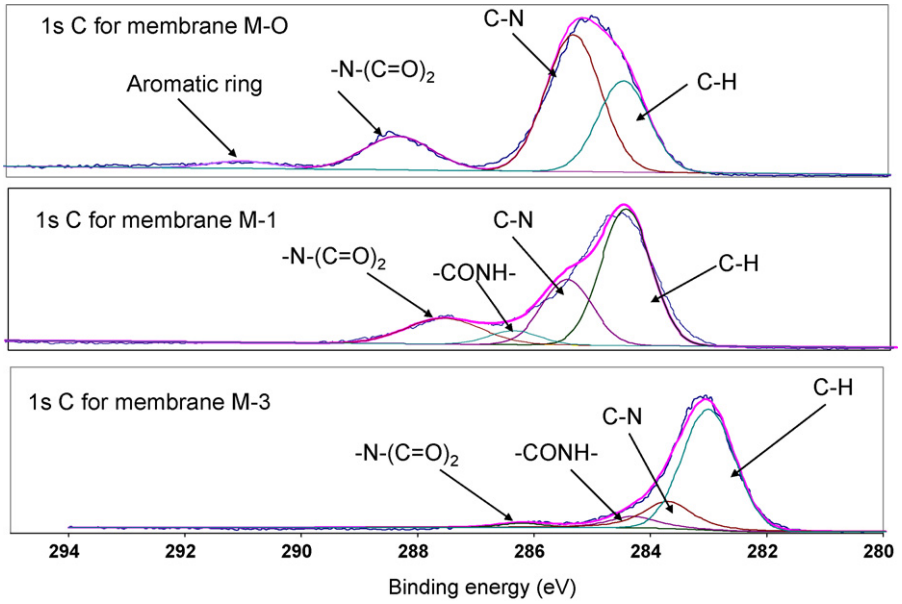

Fig. 6. XPS analysis of 1s C of the original P84 membrane M-0, diamine modified membrane M-1 and quaternary amine membrane M-3 membranes.

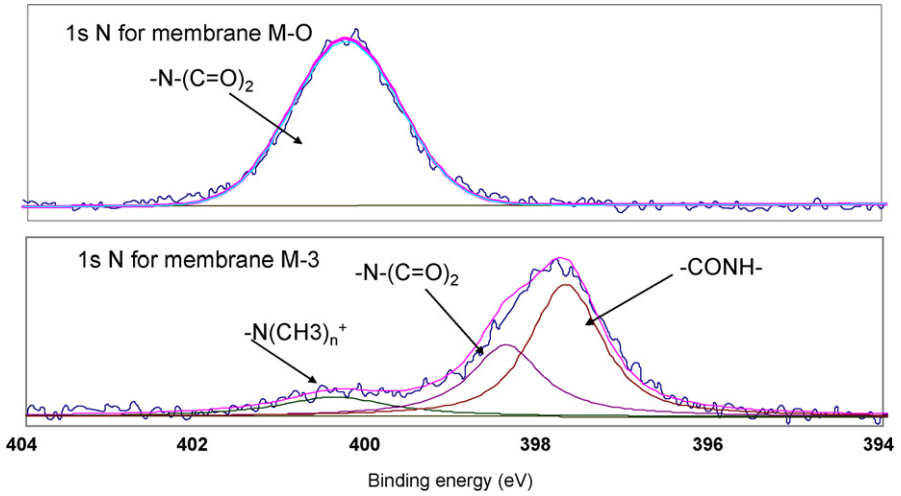

Fig. 7. XPS analysis of 1s N of the original P84 membrane M-0 and quaternary amine membrane M-3.

In addition, the functional peaks obviously shift to the right-hand side in both Figs. 6 and 7, which is the red-shift phenomenon [36], indicating the modified membrane surfaces have become easy to accept photonelectrons emitted by the X-ray source. As a result, the modified membrane surface tends to be positively charged.

Table 3 summarizes the IEC value, electric resistance and streaming (ζ) potential and PWP. Compared with the original P84 membrane, the IEC value increases from a negative value to a positive value as the modification proceeds: M-0 < M-1 < M-2, M-3. Since a higher reaction temperature with CH_3I was utilized during the fabrication of M-3 membranes, M-3 has stronger anion-

Table 3
Membrane characterization data and protein separation fluxes of different types of membranes.

	M-0	M-1	M-2	M-3
IEC value[a] (meq/m^2)	0	0.37	4.70	12.10
Electric resistance (MΩ)	9.65	7.78	6.52	5.36
Corrected ζ-potential[b] (mV) at pH 6.5	−30	+5	+12	+25
PWP[c] (m^3/m^2 s) at 5 bar	1.55E−5	1.05E−5	5.94E−6	4.71E−6
Pore size above[d] r_p = 3.9 nm	63.3%	39.9%	35.5%	28.8%
Flux of myoglobin (Mb)[e] (g/h m^2)	0.447	1.790	2.238	5.818

[a] IEC is the ion exchange capacity.
[b] The ζ-potentials were measured in a 20 mM HCl–tris buffer and corrected by 0.1 M KCl.
[c] PWP is the pure water permeation tests.
[d] Read from Fig. 11.
[e] The protein separation tests were performed at 100 mA current.

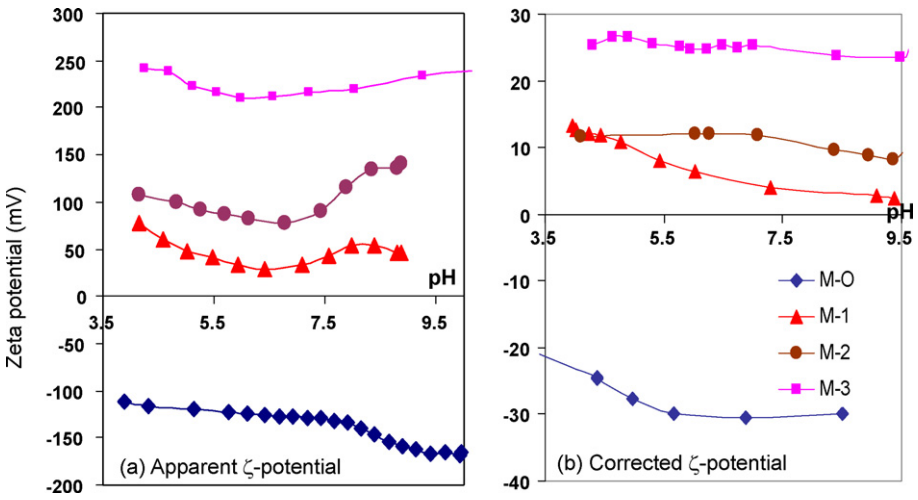

Fig. 8. ζ-potential of four types of membranes from different modification steps.

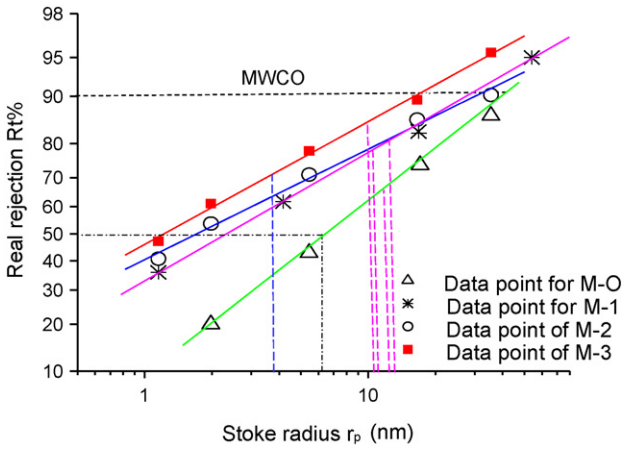

Fig. 9. Real rejection rates of four types of membranes.

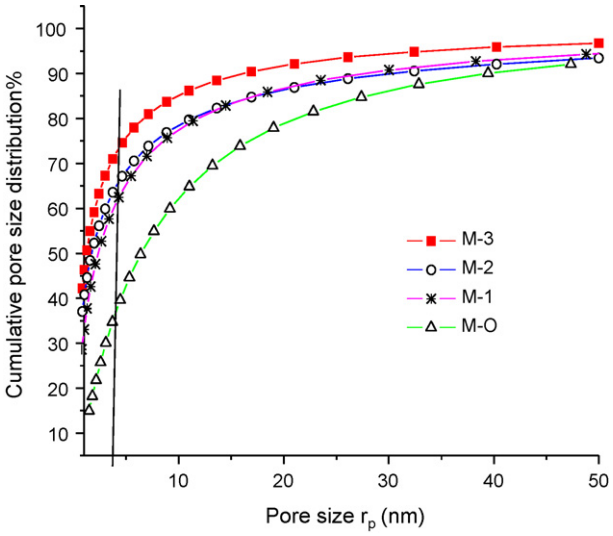

Fig. 11. Cumulative pore size distributions.

exchangeable characteristics due to quaternary amine groups. Table 3 confirms this hypothesis because M-3 has a much higher IEC value than M-2. Correspondingly, the apparent ζ-potentials of these four membranes increase following the same trend, i.e. $\zeta_{M\text{-}0} < \zeta_{M\text{-}1} < \zeta_{M\text{-}2} < \zeta_{M\text{-}3}$ as shown in Fig. 8. Although streaming ζ-potential is a function of pH, the titration curves by the streaming potential analyzer shows that M-1, M-2 and M-3 have positive apparent ζ-potentials in the range of pH 6.5–8.5, which means that M-1, M-2 and M-3 are all positively charged under this pH range.

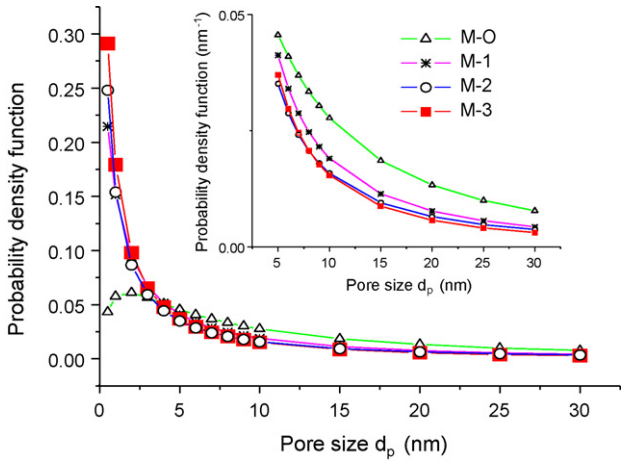

Fig. 10. Probability density functions of pore size distributions.

As displayed in Fig. 8, the apparent ζ-potential of the original P84 membrane (M-0) is negative in the range of pH 4–10. This indicates that the unmodified P84 polymer is slightly negatively charged in the observed range, which is due to the unshared electron pair in imide group. Its high absolute value is mainly due to the surface conductivity on the membrane surface [31]. Similarly, the apparent ζ-potential values of M-1, M-2 and M-3 shown in Fig. 8(a) are also enlarged due to the same reason. As mentioned in the Section 2, when a rather dilute buffer solution is used, the surface conductivity has to be considered and the corrected ζ-potential should be calculated through Eq. (4). After the correction of surface conductivity, the corrected ζ-potentials of 1 mM KCl buffers were also given in Fig. 8(b). Different absolute values were displayed in (a) and (b). However, the same trend can be observed from them: compared with M-0, the ζ-potentials of M-1 and M-2 were more positive, and that of M-3 was extremely stable at a higher positive level with various pH. This is probably due to the formation of quaternary amine, thereby induces a higher density of positive charge at the M-3 surface. Since a higher density of surface charge will suppress the pH influence on streaming potentials [37], M-3 has quite

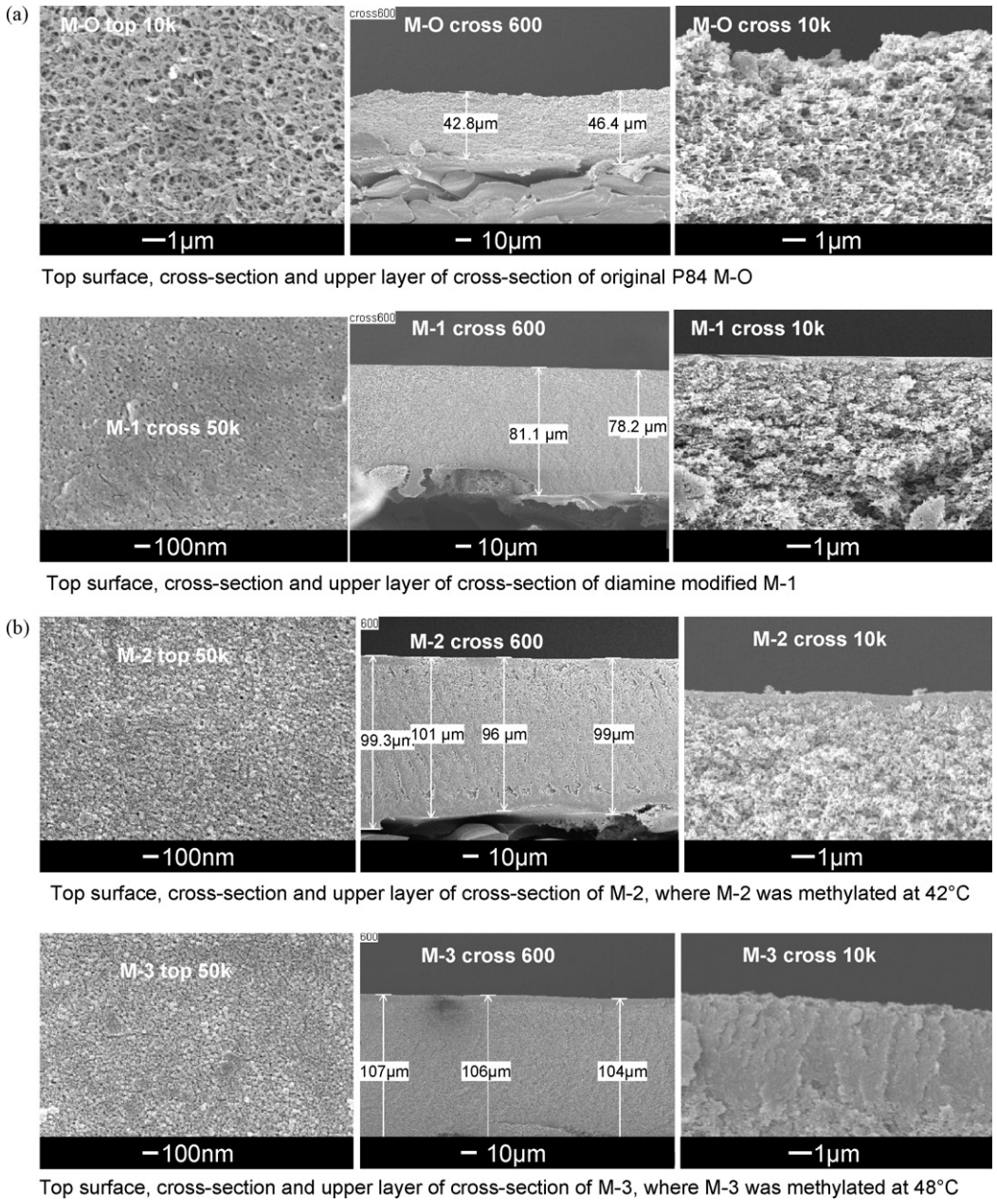

Fig. 12. (a) Comparison of FESEM images of four types of membranes from different modification steps: M-0 and M-1. (b) Comparison of FESEM images of four types of membranes from different modification steps: M-2 and M-3.

stable ζ-potential values. On the other hand, because the number of charged sites in per membrane volume increases with the proposed chemical modifications, a decrease in electric resistances (R) was observed in the order of resistance: $R_{M\text{-}0} > R_{M\text{-}1} > R_{M\text{-}2} > R_{M\text{-}3}$. As a result of the lower electric resistance, the higher membrane conductivity, solute mobility and protein mass transfer should be observed in a highly charged membrane. Therefore, according to this prediction, M-3 might have a superior performance among these membranes.

3.2. Pure water permeation (PWP) and morphological changes during modifications

Table 3 shows the PWP values of these four membranes. Their PWP decreases with chemical modifications, and M-3 has the lowest PWP. The decreased PWP indicates that their pore sizes become smaller with modifications. Since the PWP value is strongly related to membrane structure such as pore size, porosity and intra-pore connections [38], the PWP value may indirectly provide the information about porous flow channels within a membrane. The low PWP values of M-3 may be resulted from the effects of the insertion of diamine molecules and bulk groups $-N(CH_3)_3^+$ in a confined pore space.

Fig. 9 shows the mean pore sizes and pore sizes corresponding to MWCOs of the four membranes. It can be seen that the mean pore size follows the sequence of: M-0 > M-1 > M-2 > M-3, whereas the MWCOs follows: M-0 > M-1, M-2 > M-3. These tendency indicates that the pore size decreases when the modification proceeds, which is consistent with the PWP results. Fig. 10 displays the probability density functions. It can be seen clearly that there is a huge amount of small pores produced from the modification process and this leads to the density function moving closer to the y-axis as the modification proceeds. This phenomenon arises from the fact

Table 4
Mechanical strength and stability of membrane M-3.

Membrane ID	Tensile strength (MPa)	Young's modulus (Mpa)
M-3 immersed in water one week	15.18	475.53
M-3 immersed in 0.1 M HCl two weeks	13.00	420.56
M-3 under pH 4 electric field one week	14.24	443.39
M-3 under pH 10 electric field one week	15.06	397.01

that the proposed chemical modifications reduce pore radius and change membrane morphology.

As has been discussed in our previous work [13], protein molecules should not be regarded as infinitesimal in its dimensions. In order to offset the influence of small pores in membrane characterizations, a term called the "effective pore size" was proposed, concerning the minimum pore size allows protein molecules passing through. For Mb, this effective pore size is $r = 3.9$ nm [13]. Hence, the pore size which is smaller than the effective pore size will be removed from the calculation of the mean pore size, and the percentage of effective pores above this value will be counted. Fig. 11 shows the cumulative pore size distributions and demonstrates again that the amount of small pores increases after the modification process. It can be found that the percentage of pores (F_p) which is bigger than 3.9 nm (the minimal pore radius for Mb to pass through) [13] occupies 63.5%, 40.0%, 35.5% and 28.8% of the pores of the membranes M-0, M-1, M-2 and M-3, respectively.

Fig. 12 shows the FESEM images of the original and the as-modified flat membranes in dry conditions. The pore sizes of top surfaces display an obvious trend as follows: M-0 > M-1 > M-2 > M-3, which is consistent with the trends observed in PWP and pore size distribution. Interestingly, the chemically modified membranes become thicker as follows: M-0 < M-1 < M-2 < M-3 as shown in the cross-section images. This may be due to the swelling of the aminated polymer when the post-treatment was conducted in acidic or alkaline water solutions or may be due to self repulsion of charged molecules. The other possible factor might be due to the insertion of methyl groups of quaternary amine into the top surface during the methylation. From the 10k magnification images of the top layer of the cross-section, it can be clearly seen that the modification process densifies the top layer. In addition to the FESEM observation, it is noticed that "gelation" apparently occurs at the membrane top surface after methylation. Under FESEM the gelation layer has a similar image as a dense membrane but it is transparent under naked eyes. It is known that a dense membrane has no pores; it does not allow macro-molecules to pass through. On the contrary, a gel does not hinder the mass transfer of proteins and other macromolecules [39,40]. Thus, the "denser" layer observed in Fig. 12 for M-3 is a dried gel. It looks denser because of the contraction of a swelled structure during freeze drying to prepare samples for SEM.

3.3. Mechanical strength and stability of modified membrane

Generally, the P84 polymer is suggested to be used under pH 2–10, because the imide group can be hydrolyzed by some extreme acidic and caustic solution. The mechanical strength of the membrane becomes questionable, particularly after opening the imide ring. Hence the mechanical strength and stability of the membrane M-3 were tested by the method given in Section 2.4. Newly prepared M-3, M-3 between chambers 1 and 2, M-3 between 3 and 4 and M-3 immersed in acid were compared by tensile strength and Young's modulus. As shown in Table 4, the M-3 membranes facing chamber 1 and chamber 4 did not show a significant reduce in tensile strength and in Young's modulus after operating under an electric field for one week. However, comparing to the newly prepared M-3, the M-3 immersed in acid displayed a 13% drop in tensile strength. This obvious effect of HCl verifies the suggested pH range of applying P84 polymer is reasonable. Therefore, the modified M-3 membrane operated under conditions given in Fig. 2 possesses a reasonable mechanical strength and acceptable stability for daily operations.

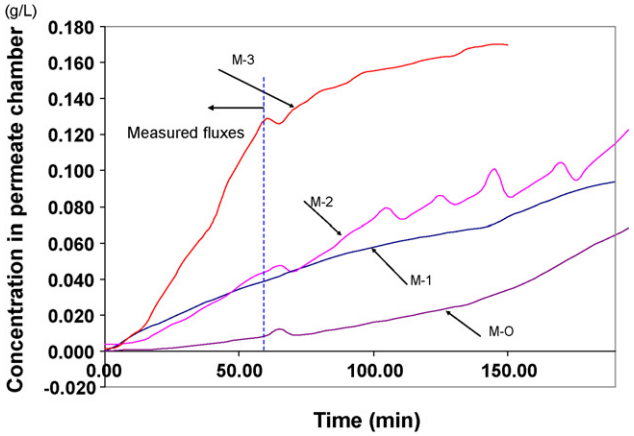

Fig. 13. Protein separation fluxes monitored by a UV–vis spectrometer.

3.4. Protein separation performance

Fig. 13 shows the myoglobin (Mb) concentrations in the 2nd chamber tested by an on-line UV–vis spectrometer for these four membranes, and Table 3 summarizes their Mb fluxes. The membrane M-3 has the highest flux, the membranes M-2 and the M-1 have intermediate fluxes, while the original P84 membrane M-0 has the lowest flux. Quantitatively, the M-3 (which was methylated at 48 °C) has a flux 2.5 times of the M-2 (which methylated at 42 °C) and 13 times of M-0. This implies that the flux is strongly related to membrane surface ζ-potential. This phenomenon corroborates well with our previous experiments that membrane surface ζ-potential facilitates protein flux [12,13] as well as the theoretical predictions by, Ennis and Anderson [41]. As can be seen from both experimental results and theoretical derivations, a charged cylindrical pore exerts positive effects to protein mass transfer in electrophoresis. Hence, membranes with a higher ζ_w will dramatically increase the mobility of counter-ion proteins in an IEM-FFIEF process [42]. This is particularly true when protein particles has a much smaller surface ζ-potential ζ_s than the pore wall potential ζ_w ($\zeta_s \ll \zeta_w$). As a consequence, ζ_w will be the dominant factor that affects the mobility μ, thus the flux.

Normally, pore size is a dominant factor influencing the flux in a UF process. A larger pore will result in a higher flux in most hydraulic pressure driven UF processes. However, in this study, the protein separation flux behaves oppositely from the above common sense: an increase in flux is observed as the pore size decreases. This is due to the fact that the boundary effects of charged membrane have exceeded the steric hindrance of pores and the higher flux of M-3 is a result of the competition between boundary effects and steric hindrance. The flux results shown in Fig. 13 indicate that the increased surface charge of a membrane is another important factor to improve the mass transfer of charged macro-molecules across the membrane.

Fig. 14 shows the protein compositions analyzed by HPLC in different chambers when applying M-3 in the IEM-FFIEF system. Only two peaks for myoglobin appear at the permeate side and no lysozyme peak can be found in the chamber 2, and only a trivial amount of myoglobin appears in the chamber 1. Meanwhile,

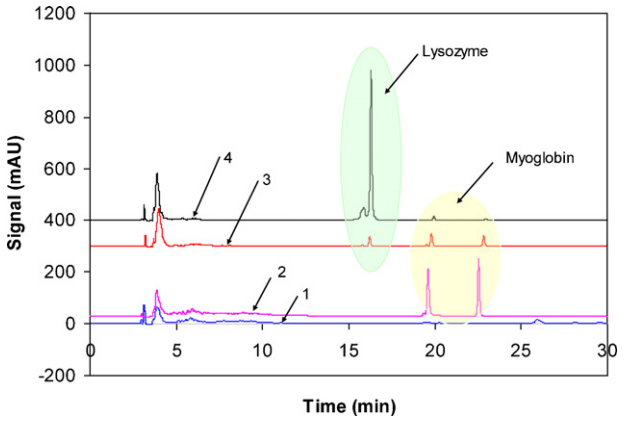

Fig. 14. HPLC results of protein separation of (Mb + Lys) in the IEM-FFIEF system where numbers 1, 2, 3 and 4 correspond to chambers 1, 2, 3 and 4, respectively.

most of lysozyme appears in the chamber 4, and a very small amount of myoglobin can be observed. The positively charged Lys molecules might be rejected by the anion-exchange membrane or might migrate to the chamber 4. As a result of boundary effect, the rejection or migration of lysozyme takes place depending on pore size, pore surface charge and charge carried on lysozyme molecules. When pore size is small enough, the lysozyme should be rejected by the positively charged membrane. However in this study, there are 20% pores in the M-3 and 30% pores in the M-2 bigger than the molecular size of lysozyme, therefore the migration of lysozyme to the chamber 4 is inevitable. Compared to the M-3, the performance test for the M-2 has a similar HPLC results. The selectivity of the membranes M-2 between chambers 2 and 3 was infinitely large, but the flux was much smaller. This performance results imply that the purity and concentration of individual chamber (2 and 4) can reach to an extremely high level if a suitable anion charged membrane is used.

4. Conclusion

The objectives of this research are to (1) conduct a fundamental study on anion-exchange membrane formation and (2) develop a suitable anion-exchange membrane which can be integrated with IEM-FFIEF for enhanced protein separation. Experimental results show that amination by diamine and then methylation by methyl iodide is an effective route to produce a highly charged anion-exchange membranes based on P84 polyimide. The membrane M-3 which was methylated at 48 °C exhibits the highest and most stable separation because it possesses the highest IEC value, hence allowing anion type Mb molecules to migrate across the membrane faster. It is also found that the proposed chemical modifications reduce pore sizes and methylation by methyl iodide produces a gel-like structure with smaller pore sizes on the P84 membrane surface. This work also demonstrates that the determinant factor for the flux of IEF-FFIEF includes both surface charge and pore structure of membrane, rather than pore size only. This conclusion means that ion-exchanged membrane is rather an advantage than an impediment for the purpose of increasing protein separation fluxes in the IEM-FFIEF system.

Acknowledgements

The authors would like to thank A-star and National University of Singapore (NUS) for funding this research with the grant numbers of R-279-000-164-305 and R-279-000-249-646. Special thanks are given to Dr. L.Y. Jiang, Y. Wang and Mr. Z. Z. Zhou, for their valuable assistance.

References

[1] R. van Reis, A.L. Zydney, Membrane separations in biotechnology, Curr. Opin. Biotechnol. 12 (2001) 208.
[2] F.G. Smith III, W.M. Deen, Electrostatic double layer interactions for spherical colloids in cylindrical pores, J. Colloid Interface Sci. 78 (1980) 444.
[3] F.G. Smith III, W.M. Deen, Electrostatic effects on the partitioning of spherical colloids between dilute bulk solution and cylindrical pores, J. Colloid Interface Sci. 91 (1993) 571.
[4] A.L. Zydney, Protein separations using membrane filtration: new opportunities for whey fractionation, Int. Dairy J. 8 (1998) 243.
[5] A.L. Zydney, N.S. Pujar, Protein transport through porous membranes: effects of colloidal interactions, Colloid Surf. A 138 (1998) 133.
[6] S. Galier, H.R. Balmann, Study of the mass transfer phenomena involved in an electrophoretic membrane contactor, J. Membr. Sci. 194 (2001) 117.
[7] J. Watson, Continuous, free-flow electrophoresis: a modified approach, Sep. Technol. 4 (1994) 239.
[8] P. Wenger, P. Javet, Isoelectric focusing using non-amphoteric buffers in free solution. I. Determination of stable concentration profiles, J. Biochem. Biophys. Methods 13 (1986) 259.
[9] van Nunen, C.A.P.M., Design of Large Scale Membrane, Electrophoresis Module for Separation of Proteins, Ph.D. thesis, University of Eindhoven, 1997.
[10] M. Bier, T. Long, Recycling isoelectric focusing: use of simple buffer, J. Chromatogr. 604 (1992) 73.
[11] M. Bier, Recycling isoelectric focusing and isotachophoresis, Electrophoresis 19 (1998) 1057.
[12] J.H. Cheng, Y. Li, T.S. Chung, S.B. Chen, W.B. Krantz, High performance protein separation by ion exchange membrane partitioned free flow isoelectric focusing system, Chem. Eng. Sci. 63 (2008) 2241.
[13] J.H. Cheng, T.S. Chung, S.H. Neo, Investigation of mass transfer in the ion-exchange membrane partitioned free-flow isoelectric focusing system (IEM-FFIEF) for protein separation, Electrophoresis 30 (2009) 2600.
[14] H. Kawabe, Amination of chloromethylated polystyrene with amino alcohols, Bull. Chem. Soc. Jpn. 54 (1981) 2886.
[15] A. Warshawsky, O. Kedem, Polysulfone-based interpolymer anion exchange membrane, J. Membr. Sci. 53 (1990) 37.
[16] T. Gullinkala, I. Escobar, Study of the hydrophilic-enhanced ultrafiltration membrane, Environ. Prog. 27 (2008) 210.
[17] H. Xu, X.Z. Hu, Preparation of anion exchangers by reductive amination of acetylated crosslinked polystyrene, React. Funct. Polym. 42 (1999) 235.
[18] L. Wu, T.W. Xu, W.H. Yang, Fundamental studies of a new series of anion exchange membranes: membrane prepared through chloroacetylation of PPO followed by quaternary amination, J. Membr. Sci. 286 (2006) 185.
[19] H. Xu, X.Z. Hu, A novel way to prepare anion exchangers based on crosslinked polystyrene, Polym. Bull. 40 (1998) 47.
[20] A. Hartwig, M. Mulder, C.A. Smolders, Surface amination of poly(acrylonitrile), Adv. Colloid Interface Sci. 52 (1994) 65.
[21] The carcinogenic substance regulations, No. 879 HMSO London.
[22] List of controlled toxic industrial waste, Singapore.
[23] P.S. Tin, Y.C. Xiao, T.S. Chung, Polyimide-carbonized membranes for gas separation: structural, composition, and morphological control of precursors, Sep. Purif. Rev. 35 (2006) 285.
[24] X. Li, M.R. Coleman, Functionalization of carbon nanofibers with diamine and polyimide oligmer, Carbon 46 (2008) 1115.
[25] X.Y. Qiao, T.S. Chung, Diamine modification of P84 polyimide membranes for pervaporation dehydration of isopropanol, AIChE J. 52 (2006) 3462.
[26] E. Baer, An introduction to high performance polymer, High Perform. Polym. 11 (1990) 395.
[27] B.T. Low, Y.C. Xiao, T.S. Chung, Y. Liu, Simultaneous occurrence of chemical grafting, cross-linking, and etching on the surface of polyimide membranes and their impact on H_2/CO_2 separation, Macromolecules 41 (2008) 1297.
[28] L. Shao, L. Liu, S.X. Cheng, Y.D. Huang, J. Ma, Comparison of diamino cross-linking in different polyimide solutions and membranes by precipitation observation and gas transport, J. Membr. Sci. 312 (2008) 174.
[29] N. Peng, T.S. Chung, K.Y. Wang, Macrovoid evolution and critical factors to form macrovoid-free hollow fiber membranes, J. Membr. Sci. 318 (2008) 363.
[30] F.A. Carey, Organic Chemistry, 6th edition, Mc GRAW HILL, New York, 2006, p. 967.
[31] M.D. Afonso, Surface charge on loose nanofiltration membranes, Desalination 191 (2006) 262.
[32] K.Y. Wang, T.S. Chung, The characterization of flat composite nanofiltration membranes and their applications in the separation of cephalexin, J. Membr. Sci. 247 (2005) 37.
[33] K.Y. Wang, T. Matsuura, T.S. Chung, W.F. Guo, The effects of flow angle and shear rate within the spinneret on the separation performance of poly(ethersulfone) (PES) ultrafiltration hollow fiber membranes, J. Membr. Sci. 240 (2004) 67.
[34] R.J. Simpson, Purifying Proteins for Proteomics: A Laboratory Manual, Gold Spring Harbor, New York, 2004, p. 659.
[35] G. Socrates, Infrared, Raman Characteristic Group Frequencies, John Wiley & Sons, New York, 2004, p. 38 or p. 146.
[36] G. Beamson, D. Briggs, High Resolution XPS of Organic Polymer: The Scienta ESCA300 Database, Wiley, New York, 1992.
[37] C.M. Wu, T.W. Xu, W.H. Yang, A new inorganic–organic negatively charged membrane: membrane preparation and characterizations, J. Membr. Sci. 224 (2003) 117.

[38] Y. Li, T.S. Chung, Exploration of high sulfonated polyethersulfone as a membrane material with the aid of dual layer hollow fiber fabrication technology for protein separation, J. Membr. Sci. 309 (2008) 45.
[39] D. Garfin, S. Ahuja, Handbook of Isoelectric Focusing and Proteomics, Academic Press, 2005, p. 127.
[40] R.A. Mosher, D.A. Saville, W. Thormann, The Dynamics of Electrophoresis, VCH publishers, New York, 1992 (Chapter 7).
[41] J. Ennis, J.L. Anderson, Boundary effects on electrophoretic motion of spherical particles for thick double layer and low zeta potential, J. Colloid Interface Sci. 185 (1997) 497.
[42] Y.H. Su, Y.L. Liu, D.M. Wang, J.Y. Lai, M.D. Guiver, B. Liu, Increases in the proton conductivity and selectivity of proton exchange membranes for direct methanol fuel cells by formation of nanocomposites having proton conducting channels, J. Power Sources 194 (2009) 206.